Molecular and environmental cues in cardiac differentiation of mesenchymal stem cells

Ramkisoensing, A.A.

CHAPTER VII

ENGRAFTMENT PATTERNS OF HUMAN ADULT MESENCHYMAL STEM CELLS EXPOSE ELECTROTONIC AND PARACRINE PRO-ARRHYTHMIC MECHANISMS IN MYOCARDIAL CELL CULTURES

Arti A. Ramkisoensing, MSc, MD; Saïd F.A. Askar, MSc*, Douwe E. Atsma, MD, PhD; Martin J. Schalij, MD, PhD; Antoine A.F. de Vries, PhD*; Daniël A. Pijnappels, PhD*.*

*Equal Contribution

Circ Arrhythm Electrophysiol. 2013 Apr;6(2):380-91.

ABSTRACT

Background: After intramyocardial injection, mesenchymal stem cells (MSCs) may engraft and influence host myocardium. However, engraftment rate and pattern of distribution are difficult to control *in vivo*, hampering assessment of potential adverse effects. In this study, the role of MSCs engraftment patterns on arrhythmicity in controllable *in vitro* models is investigated.

Methods&Results: Co-cultures of 4×10^5 neonatal rat cardiomyocytes (nrCMCs) and 7% or 28% adult human (h) MSCs in diffuse or clustered distribution patterns were prepared. Electrophysiological effects were studied by optical mapping and patch-clamping. In diffuse co-cultures, hMSCs dose-dependently decreased nrCMC excitability, slowed conduction and prolonged APD_{90}. Triggered activity (14% vs. 0% in controls) and increased inducibility of reentry (53% vs. 6% in controls) were observed in 28% hMSC co-cultures. MSC clusters increased APD_{90}, slowed conduction locally, and increased reentry inducibility (23%), without increasing triggered activity. Pharmacological heterocellular electrical uncoupling increased excitability and conduction velocity to 133% in 28% hMSC co-cultures, but did not alter APD_{90}. Transwell experiments showed that hMSCs dose-dependently increased APD_{90}, APD dispersion, inducibility of reentry and affected specific ion channel protein levels, while excitability was unaltered. Incubation with hMSC-derived exosomes did not increase APD in nrCMC cultures.

Conclusions: Adult hMSCs affect arrhythmicity of nrCMC cultures by heterocellular coupling leading to depolarization-induced conduction slowing and by direct release of paracrine factors that negatively affect repolarization rate. The extent of these detrimental effects depends on the number and distribution pattern of hMSCs. These results suggest that caution should be urged against potential adverse effects of myocardial hMSC engraftment.

INTRODUCTION

Over the past decade, stem cell therapy has been subject of studies aiming to improve function of damaged hearts. Particularly mesenchymal stem cells (MSCs) have been of interest in these efforts.[1,2] In spite of the fact that only low percentages of injected MSCs survive and integrate in damaged myocardium, therapeutic effects have been found in pre-clinical studies.[3,4] Moreover, genetically modified MSCs have also been investigated as vehicles of biological functions such as biological pacemakers.[5] Also, intramyocardial transplantation of bone marrow-derived cells, including human (h) MSCs, into diseased human myocardium has been shown to improve cardiac function.[6] These positive effects on cardiac function are believed to be mainly mediated by paracrine factors released from the transplanted cells.[7] Therefore, increasing engraftment rate to improve the therapeutic effects of transplanted cells seems a logical step and is indeed the focus of current stem cell research.[8,9] However, the risk of adverse effects with higher engraftment rates in largely uncontrolled engraftment patterns is unknown. The number of transplanted cells that actually engrafts and their distribution patterns are difficult to regulate. Only few studies have focused on these aspects. Fukushima *et al.* showed that engraftment patterns of transplanted bone marrow cells may depend on administration route, *i.e.* direct intramyocardial injection resulted in a more clustered distribution than intracoronary infusion.[10] Such clustering may lead to formation of local conduction blocks, potentially facilitating reentrant tachyarrhythmias. Additionally, *in vitro* studies by Chang *et al.* have indicated that administration of hMSCs to myocardial cell cultures may indeed increase pro-arrhythmic risk.[11] However, besides indirect implications that electrotonic coupling of MSCs with host cardiomyocytes may be responsible for their pro-arrhythmic effects, the mechanisms underlying MSC-dependent arrhythmogeneity remain unknown. Also, insights concerning differences between pro-arrhythmic effects of distinct engraftment profiles of MSCs are still limited. As a result, further investigation of potentially pro-arrhythmic actions of hMSCs is required. Such studies are especially important to improve therapeutic efficacy and to contain the hazardous potential of MSC therapy in the heart. Therefore, this study aimed to investigate the effects of engraftment characteristics of MSCs (*i.e.* different numbers and distribution patterns) on arrhythmicity using controllable *in vitro* models. We found that hMSCs can indeed be pro-arrhythmic depending on their number and distribution pattern and that direct contact between neonatal rat ventricular cardiomyocytes (nrCMCs) and hMSCs as well as paracrine effects of hMSCs on nrCMCs are important contributors to the pro-arrhythmic effects of hMSCs. The results of this study suggest that caution is warranted against potential pro-arrhythmic effects of MSC transplantation in cardiac tissue. The acquired knowledge about the mechanisms by which hMSCs can

cause arrhythmias may help to develop strategies how to increase the safety and efficacy of intramyocardial hMSC administration.

MATERIALS AND METHODS

A more detailed description of the materials and methods can be found in the Supplemental Material, which also includes methods of immunocytological stainings, western blot, dye-transfer and patch-clamp experiments.

ISOLATION, CULTURE AND CHARACTERIZATION OF HMSCS

Human tissue samples were collected after having obtained written informed consent of the donors and with the approval of the medical ethics committee of Leiden University Medical Center (LUMC). The procedures used in this investigation conformed to the Declaration of Helsinki. Human MSCs were purified from leftover bone marrow samples derived from adult ischemic heart disease patients (n=4 donors). hMSCs were characterized by immunophenotyping and by their adipogenic and osteogenic differentiation potential as described in the online supplement.

ISOLATION AND CULTURE OF NRCMCS

All animal experiments were approved by LUMC's animal experiments committee and conform to the Guide for the Care and Use of Laboratory Animals, as stated by the US National Institutes of Health (10236).[12] Briefly, hearts were rapidly excised from isoflurane-anesthetized animals, the ventricles were minced into pieces and dissociated by treatment with collagenase type I (450 units/mL; Worthington Biochemical, Lakewood, NJ). The myocardial cells were pre-plated to minimize contamination of the nrCMC cultures with non-cardiomyocytes. Purified myocardial cells were plated on fibronectin (Sigma-Aldrich Chemie, Zwijndrecht, the Netherlands)-coated coverslips in 24-wells plates (Corning Life Sciences, Amsterdam, the Netherlands) at a density of $1\text{-}4\times10^5$ cells/well depending on the experiment. All cultures were treated with 10 µg/mL mitomycin-C (Sigma-Aldrich Chemie) to halt proliferation of endogenous fibroblasts.

CO-CULTURE OF NRCMCS AND CLUSTERED OR DIFFUSELY SPREAD HMSCS

To investigate the effects on arrhythmicity of myocardial engraftment of hMSCs in different patterns and doses, co-cultures of nrCMCs and hMSCs were prepared. To mimic a diffuse engraftment pattern, 4.0×10^5 nrCMCs were mixed with 2.8×10^4 (7%) or 1.12×10^5 (28%) hMSCs and added onto coverslips in wells of a 24-well cell culture plate. To mimic a clustered engraftment pattern, rings with an outer

diameter of 15 mm and a central inner diameter of 3 or 6 mm were lasered in Parafilm M (Bemis Company, Neenah, WI, USA) and attached to the coverslips. Next, hMSCs were applied in these circles (3 mm: 2.8×10^4 cells or 6 mm: 1.12×10^5 cells). After attachment, the Parafilm was removed and the attached hMSCs were overlaid with 4.0×10^5 nrCMCs.

Optical mapping

Electrophysiological parameters were determined by optical mapping as described previously.[13] Cultures were loaded with di-4-ANEPPS (Invitrogen, Breda, the Netherlands) for 10 min at 37°C. Cultures were then given fresh DMEM/F12 (Invitrogen) and optically mapped using the Micam Ultima-L optical mapping system (Scimedia USA, Costa Mesa, CA).

Analysis of the influence of paracrine factors on electrophysiological parameters of nrCMC cultures

Mitomycin-C-treated adult hMSCs were seeded in 24-well plate transwell inserts (Corning Life Sciences). To mimic as much as possible the conditions of the non-transwell experiments, the inserts contained 2.8×10^4 or 1.12×10^5 hMSCs and were placed above 4.0×10^5 mitomycin-C-treated nrCMCs seeded on fibronectin-coated coverslips. Control cultures consisted of nrCMC cultures with no, empty or nrCMC (1.12×10^5 cells)-filled transwell inserts. In addition, exosomes were derived from hMSCs[14,15] and incubated with nrCMCs cultures for 9 days.

Statistics

Experimental data was analyzed by the Mann-Whitney-U test for direct comparisons, or the Wilcoxon signed-rank test for paired observations. For multiple comparisons, the Kruskal-Wallis test with Dunn' s *post-hoc* correction was used. Experimental results were expressed as mean±standard deviation (SD) for a given number (n) of observations. Statistical analysis was performed using SPSS 16.0 for Windows (SPSS, Chicago, IL). Differences were considered statistically significant at $P<0.05$.

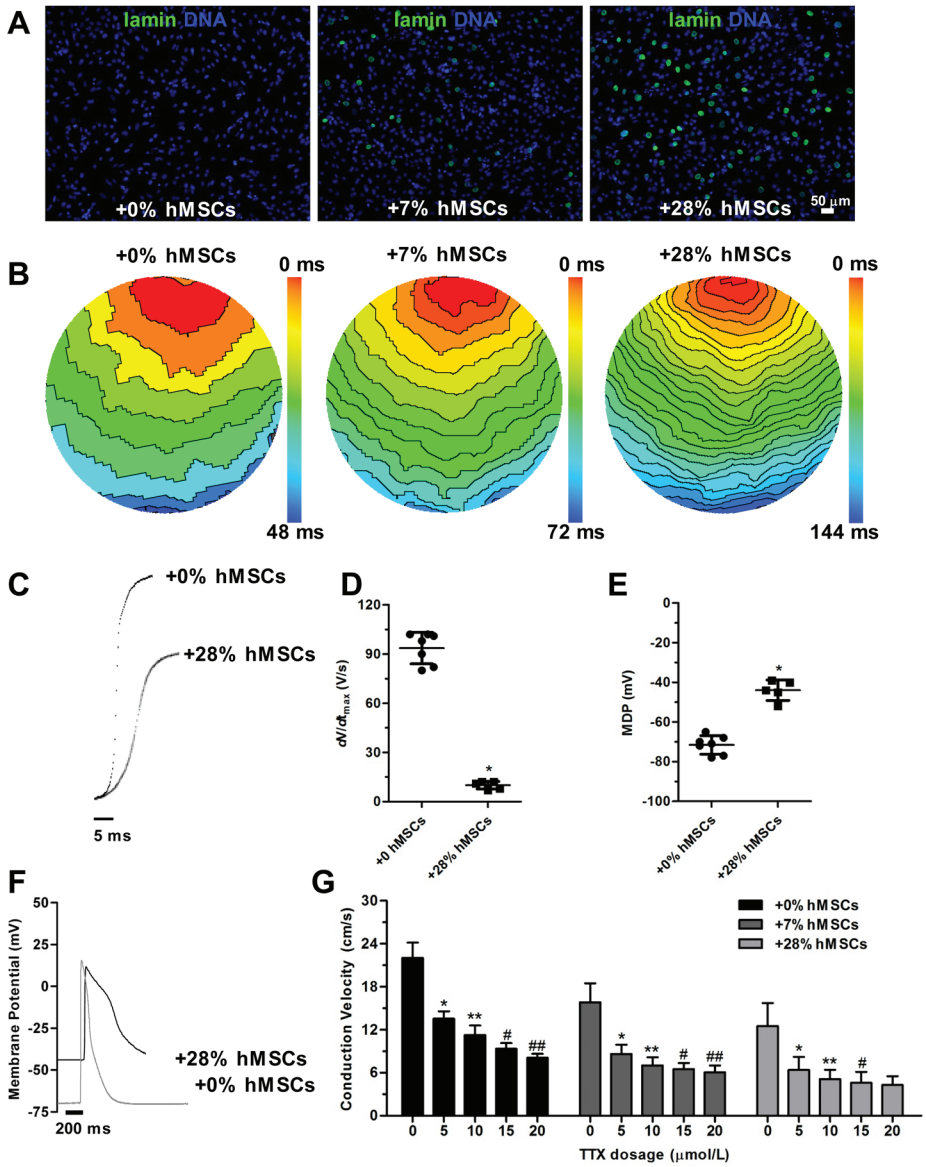

Figure 1. Conduction slowing and decreased excitability in myocardial cell cultures containing diffusely spread hMSCs. (A) Fluorescent microscopy images of myocardial cell cultures containing 0%, 7% or 28% hMSCs stained for human-specific lamin A/C (green). (B) Activation maps of myocardial cell cultures with 0%, 7% or 28% added hMSCs. Isochrones: 6 ms. (C) Typical action potential upstroke traces recorded with current-clamp in nrCMCs in a control culture or in culture with 28% hMSCs. (D) Quantification of maximum depolarization rate (dV/dt_{max}). *P<0.05 vs. 0% hMSCs. (E) Quantification of MDP recorded in

nrCMCs. *P<0.05 vs. 0% hMSCs. (F) Typical voltage traces from nrCMCs in myocardial cell cultures containing 0% or 28% hMSCs. (G) Quantification of the effect of stepwise increasing TTX dose. *P<0.05 vs. 0 µmol/L TTX, **P<0.05 vs. 5 µmol/L TTX, $^{\#}P$<0.05 vs. 10 µmol/L TTX, $^{\#\#}P$<0.05 vs. 15 µmol/L TTX.

RESULTS

DIFFUSELY SPREAD HMSCS DOSE-DEPENDENTLY DECREASE CONDUCTION VELOCITY (CV) AND EXCITABILITY IN MYOCARDIAL CELL CULTURES

Adult hMSCs used in this study fulfilled established identity criteria, as shown in the Online Supplement (Supplemental Figure 1). The pro-arrhythmic effects of hMSCs were first investigated in co-cultures of hMSCs and nrCMCs in which the hMSCs were evenly distributed throughout the monolayer (Figure 1A). Addition of 7% or 28% hMSCs to nrCMCs dose-dependently slowed conduction from 21.6±1.8 cm/s (0% hMSCs, n=15) to 17.1±3.1 (7% hMSCs, n=20) and 12.6±3.2 cm/s (28% hMSCs, n=64, P<0.05 between experimental groups, Figure 1B). Current-clamping of parallel cultures revealed a decrease in upstroke velocity in 28% hMSC-containing myocardial cell cultures (10±2 [n=5] vs. 94±10 V/s [n=7] in control cultures, P<0.05, Figure 1C-D). Moreover, maximal diastolic potentials (MDPs) were less negative for nrCMCs in co-culture with 28% hMSCs (-44±5 [n=5] vs. -72±5 mV [n=7] in control cultures, P<0.05, Figure 1E-F). To study the effects of diffusely spread hMSCs on excitability of nrCMC cultures, CV after administration of the voltage-gated sodium channel blocker tetrodotoxin (TTX) in increments of 5 µmol/L to 20 µmol/L was measured. In co-cultures containing 0% or 7% hMSCs, a TTX concentration-dependent decrease in CV was observed for the entire dose range (Figure 1G). However, in cultures with 28% added hMSCs, the conduction-slowing effect of TTX was saturated between 15 and 20 µmol/L (P>0.05). Moreover, the magnitude of the drop in CV by increasing TTX doses declined with increasing hMSC numbers, indicating diminished availability of Nav1.5 and thereby confirming the ability of hMSCs to decrease excitability.

HMSCS EXERT PRO-ARRHYTHMIC EFFECTS THROUGH ELECTRICAL COUPLING WITH NEIGHBORING NRCMCS

The mechanisms through which hMSCs negatively affect the excitability of nrCMCs were studied by investigating co-cultures for the expression of N-cadherin, α smooth muscle actinin (αSMA) and connexin-43 (Cx43). Adult hMSCs co-cultured with nrCMCs (n=3,000 hMSCs analyzed) stained negative for αSMA (Supplemental Figure 2A). Also, no N-cadherin was present at hMSC-nrCMC junctions (Supplemental Figure 2B). Cx43 was detected at interfaces between hMSCs and nrCMCs (Figure 2A1), but in lower quantities (20.2±2.2%, $P<0.0001$) than at nrCMC-nrCMC junctions (Figure 2A2). Functional electrical heterocellular coupling between hMSCs and nrCMCs was investigated by dye-transfer experiments. The enhanced green fluorescent protein (GFP)-labeled hMSCs showed a significantly lower dye intensity (18.7±3.0%, $P<0.001$) than adjacent, calcein-loaded nrCMCs (Figure 2B1-B2). Also, although a large fraction of GFP-positive cells had taken up the dye (84.5±4.5%), not all hMSCs were positive for calcein. The lower Cx43 levels at hMSC-nrCMC borders than at nrCMC-nrCMC interfaces were utilized to investigate the effect of heterocellular uncoupling by a low dose of the gap-junctional uncoupler 2-aminoethoxydiphenylborate (2-APB) on conduction in hMSC-nrCMC co-cultures. After administration of 2 μmol/L 2-APB, CV in 19 co-cultures of nrCMCs and 28% hMSCs rose to 133±16% of the values measured before 2-APB addition (Figure 2C-D), whereas vehicle-treated (0.01% DMSO, n=5) cultures showed no significant change (*i.e.* CV post 0.01% DMSO was 104±8% of CV before 0.01% DMSO). 2-APB increased action potential upstroke velocity from 10±3 to 29±7 V/s (n=4, $P<0.05$). Furthermore, negativity of MDP of nrCMCs increased by 33% to -59±4 mV ($P<0.05$ vs. without 2-APB) while action potential duration until 90% repolarization (APD_{90}) remained unaltered by the 2-APB treatment of the co-cultures (Figure 2E). Importantly, treatment with 2 μmol/L 2-APB did not significantly affect any of these parameters in myocardial cell cultures lacking hMSCs (data not shown).

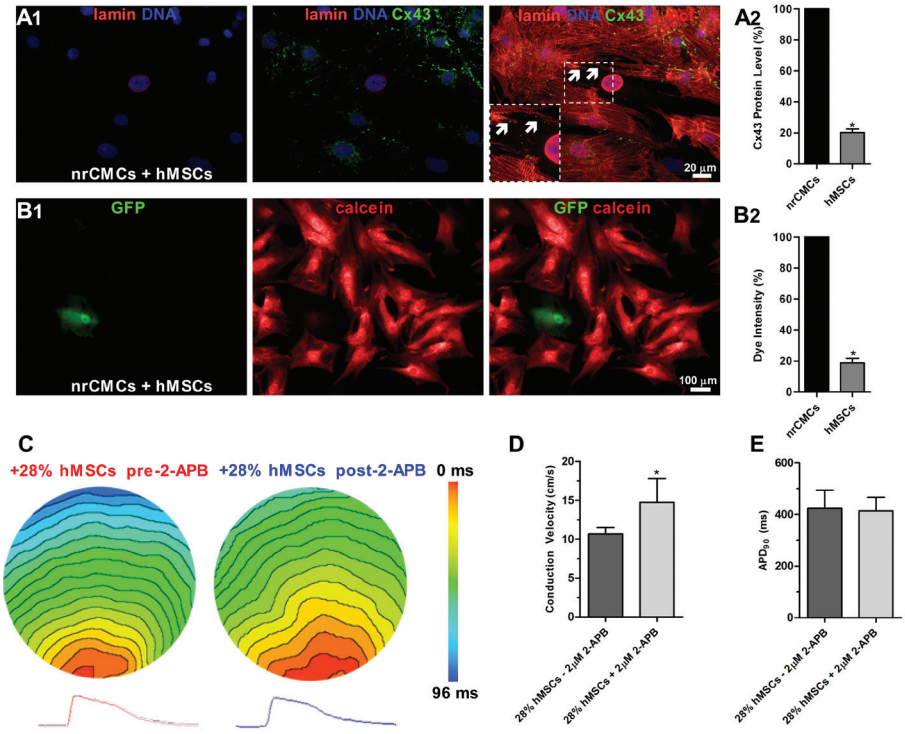

Figure 2. Diffusively spread hMSCs slow conduction through electrotonic coupling. (A1) Immunocytological analyses reveals lower Cx43 (green) levels at heterocellular interfaces between human lamin A/C-positive hMSCs (red) and α-actinin-positive nrCMCs (red/orange) than at homocellular junctions between nrCMCs. (A2) Quantification of junctional Cx43 levels at hMSC-nrCMC and at nrCMC-nrCMC interfaces. *P<0.001 vs. nrCMCs. (B1) Dye transfer from nrCMCs to GFP-positive hMSCs. (B2) Quantification of dye intensity in GFP-positive hMSCs. *P<0.001 vs. nrCMCs. (C) Activation maps before and after 2-APB administration to a myocardial cell culture containing 28% diffusely spread hMSCs. (D) 2-APB treatment increases CV in myocardial cell cultures with hMSCs. *P<0.05 vs. pre-2-APB. (E) Partial uncoupling by 2-APB does not affect repolarization in myocardial cell cultures containing evenly spread hMSCs.

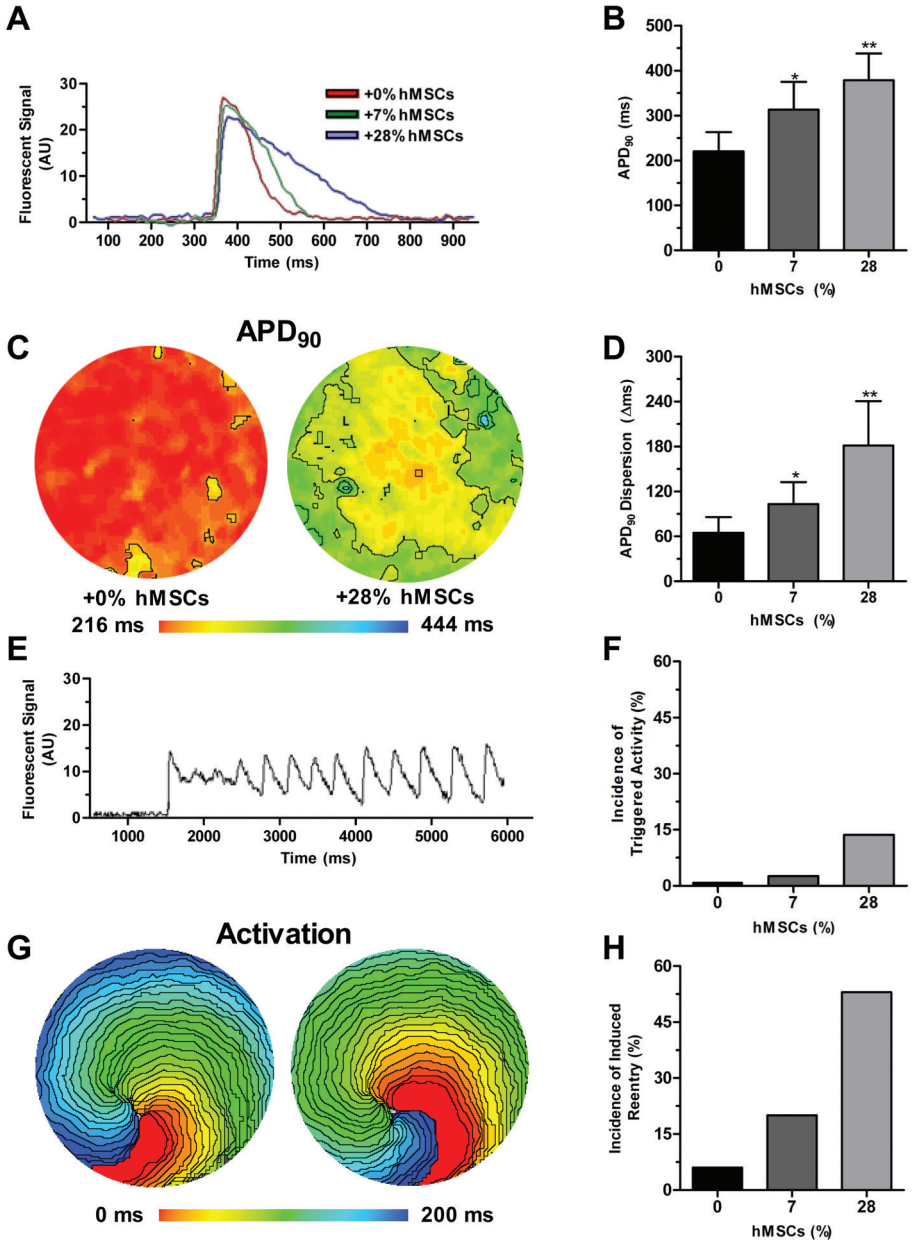

Figure 3. Slowing and dispersion of repolarization in myocardial cell cultures containing diffusely spread hMSCs. (A) Optical traces of myocardial cell cultures containing 0%, 7% or 28% hMSCs show (B) prolongation of repolarization in an hMSC dose-dependent manner. **P*<0.05 vs. 0 and 28% hMSCs, ***P*<0.05 vs. 0% and 7% hMSCs. (C) APD_{90} maps of myo-

cardial cell cultures reveal (D) an hMSC dose-dependent increase in dispersion of repolarization throughout the entire culture. *P<0.05 vs. 0 and 28% hMSCs, **P<0.05 vs. 0% and 7% hMSCs. (E) Optical trace of triggered activity in a myocardial cell culture containing 28% hMSCs. (F) Incidence of triggered activity positively correlates with the number of hMSCs in myocardial cell cultures. (G) Activation map of 2 consecutive reentrant activations during a reentrant tachyarrhythmia in a myocardial cell culture containing 28% hMSCs. (H) Inducibility of reentry increases with the number of hMSCs in myocardial cell cultures.

DIFFUSELY SPREAD HMSCS DECREASE REPOLARIZATION RESERVE AND INCREASE ARRHYTHMICITY IN MYOCARDIAL CELL CULTURES

APD_{90} was 314±61 and 379±60 ms in myocardial cell cultures containing 7% (n=24) and 28% hMSCs (n=86), respectively, compared to 221±43 ms in control cultures (n=16) (Figure 3A-B). This corresponds to an hMSC dose-dependent prolongation of repolarization time of 142% and 171%, respectively (P<0.05 between all groups). These findings were confirmed with patch-clamp experiments (APD_{60} of 186±10 ms for nrCMCs in control cultures and of 300±21 ms in cultures with 28% added hMSCs [n=5, P<0.05]). Optical mapping showed that addition of hMSCs to myocardial cell cultures caused an increase in spatial heterogeneity of repolarization (Figure 3C). In control cultures, the maximal spatial difference between APD_{90} values within the same culture was 65±21 ms (n=18). In cultures with 7% or 28% added hMSCs, APD_{90} dispersion was 103±29 (n=13) and 181±59 ms (n=17), respectively (P<0.05, Figure 3D).

Pro-arrhythmic consequences of these findings were revealed by 1 Hz stimulation, which evoked triggered activity in 14% of cultures with 28% added hMSCs (n=66, Figure 3E). Cultures containing 7% hMSCs showed a lower incidence of triggered activity (2.6%, n=39) and triggered activity was absent in control cultures (n=39, Figure 3F). Next, inducibility of reentrant arrhythmias was investigated by applying a burst stimulation protocol (Figure 3G). Reentry was induced in 6% (n=16), 20% (n=10) and 53% (n=15) of cultures containing 0%, 7% and 28% hMSCs, respectively (Figure 3H).

After confirming reproducibility of triggered activity in the same culture, the ATP-sensitive K^+-channel opener P1075 was administered, which abolished all episodes of triggered activity (n=6, Figure 4A, B). As P1075 strongly shortened APD_{90} (Figure 4C) and reduced APD dispersion (Figure 4D) without affecting CV (Figure 4E), reduced repolarization reserve and steeper spatial APD gradients caused by hMSCs seem to be crucial for inducing triggered activity.

Clustered hMSCs provide a substrate for reentry in myocardial cell cultures.

Optical mapping of myocardial cell cultures containing a central cluster of hMSCs revealed local slowing of conduction to 4.7±1.6 and 5.4±1.3 cm/s in hMSC clusters

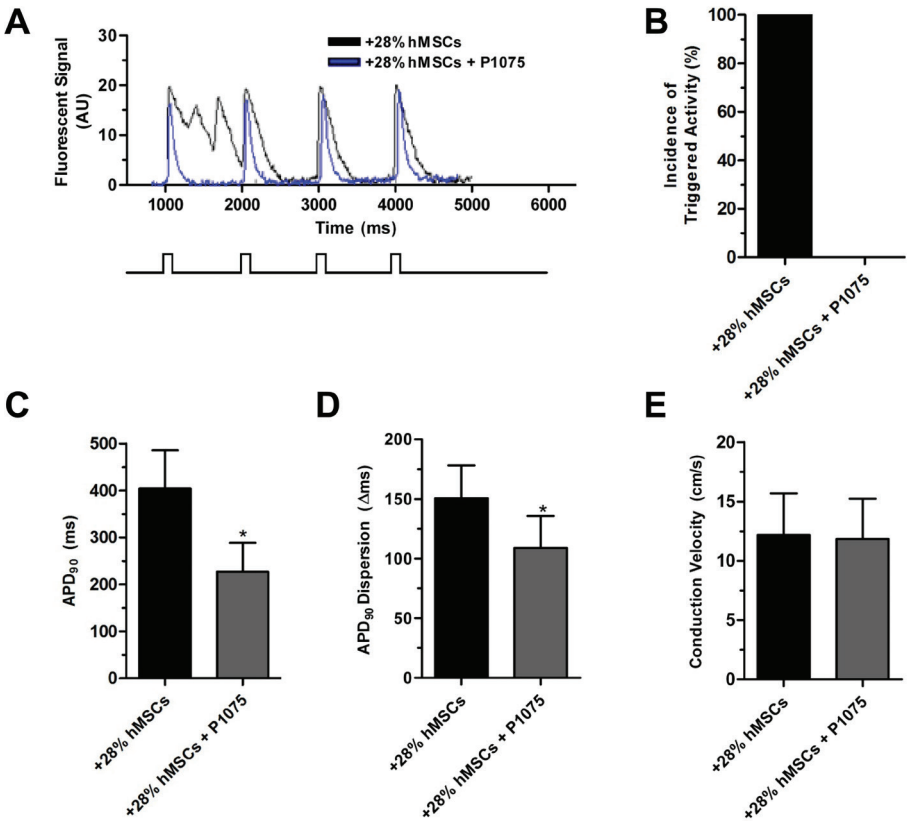

Figure 4. Increasing repolarization reserve lowers the incidence of triggered activity in nrCMC cultures containing diffusely spread hMSCs. (A) Optical traces of a myocardial cell culture with 28% hMSCs before and after P1075 administration, and corresponding (B) incidences of triggered activity. (C) Quantification of APD_{90}, (D) APD_{90} dispersion and (E) CV before and after P1075 treatment in myocardial cell cultures with 28% hMSCs. *P<0.05 vs. 28% hMSCs.

with a diameter of 3 mm (n=21) and of 6 mm (n=20), respectively (P=NS), whereas CV outside these clusters remained as high as in control cultures (22.2±1.7 and 22.4±1.8 vs. 22.4±2.3 cm/s, P=NS, Figure 5A-C). APD_{90} was prolonged inside the 3-mm hMSC clusters (333±30 vs. 254±58 ms outside, P<0.05) and inside the 6-mm hMSC clusters (343±48ms vs 310±40 ms outside, P<0.05, Figure 5D-G). Due to these local effects, APD_{90} dispersion was also increased in cultures with a 3- or 6 mm cluster of hMSCs (Figure 5D). Interestingly, APD_{90} in the ring of nrCMCs around 6-mm hMSC clusters was significantly prolonged (310±40 ms) compared to that in control cultures (245±61 ms) or in the ring of nrCMCs around

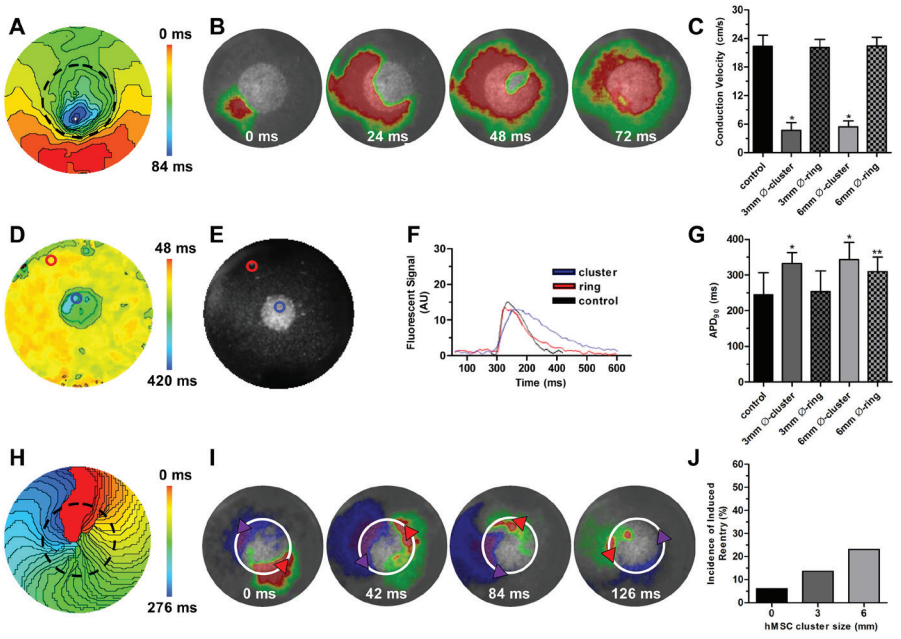

Figure 5. Myocardial cell cultures containing clustered hMSCs are substrates for reentry. (A) Typical activation map of a myocardial cell culture containing 28% hMSCs in a centrally located cluster with a diameter of 6 mm (black dotted line). (B) Pseudo-voltage map sequence projected over a picture of the same culture containing a 6-mm hMSC cluster shows (C) local conduction slowing inside the cluster. *P<0.05 vs. outer ring. (D) APD_{90} map of a culture with a 3-mm cluster of hMSCs. (E) Micrograph of a myocardial cell culture with a 3-mm hMSC cluster and (F) traces of action potentials inside (blue) and outside (red) of the hMSC cluster. (G) APD_{90} in myocardial cell cultures containing different-sized hMSC clusters. *P<0.05 vs. outer ring, **P<0.05 vs. control and outer, 3-mm ring. (H) Activation map and (I) pseudo-voltage map sequence of a reentrant tachyarrhythmia anchored at a 6-mm hMSC cluster (demarcated by black dotted and white line, respectively). (J) The incidence of induced reentry in myocardial cell cultures increases with the size of the centrally located hMSC cluster.

3-mm hMSC clusters (254±58 ms, P<0.05 vs. all, Figure 5F-G). No triggered activity was observed in any of these cultures. However, burst stimulation induced reentry in 6% of the control cultures (n=16) and in 14% (n=22) and 23% (n=30) of the cultures with 3- and 6-mm central clusters of hMSCs, respectively (Figure 5H-J). Induced reentrant arrhythmias anchored to the hMSC clusters.

HMSCS RELEASE FREE PARACRINE FACTORS THAT PROLONG REPOLARIZATION BUT DO NOT AFFECT CONDUCTION

To study a possible paracrine contribution[16] to hMSC-induced APD prolongation, transwell experiments were conducted. Transwells with inserts containing 0%, 7% or 28% hMSCs had almost identical CVs of 21.9±0.9, 22.3±1.3 and 22.9±0.7 cm/s (*P*=NS). Additionally, the conduction-slowing effect of TTX was very similar for transwell cultures containing different numbers of hMSCs (*P*>0.05, Figure 6A). However, APD_{90} was dose-dependently affected by hMSCs, as APD_{90} was 227±35 ms for controls (n=38) as compared to 300±91 and 362±88 ms for transwells with inserts containing 7% hMSCs (n=46) and 28% hMSCs (n=45), respectively (*P*<0.05, Figure 6B). Dispersion of repolarization showed a similar positive relation with hMSC numbers, with APD_{90} dispersion values of 78±23, 105±50 and 148±72 ms for transwells whose inserts contained 0%, 7% and 28% hMSCs (Figure 6C). None of the transwell cultures displayed triggered activity. However, inducibility of reentry was slightly increased from 14% (n=29) in controls to 16% (n=44) and 24% (n=38) for transwells with 7% and 28% of hMSCs, respectively (Figure 6D). Patch-clamp experiments also showed a prolonged APD in nrCMCs exposed to the secretome of 28% hMSCs (335±6 ms, n=4) compared to unexposed CMCs (193±7 ms, n=4, *P*<0.05, Figure 7A-B). However, dV/dt_{max} (104±7 V/s vs. 107±9 V/s in controls, *P*=0.72, Figure 7C) and resting membrane potential (-68±4 mV vs. -67±3 mV in controls, *P*=0.72) were unaffected by the hMSC secretome. Western blot analysis of ion channel protein levels in nrCMCs exposed to the hMSC secretome of 28% hMSCs revealed lower levels of Cav1.2 (0.43±0.01 vs. 0.22±0.04 arbitrary units, *P*<0.05) and Kv4.3 (0.26±0.04 vs. 0.22±0.04 arbitrary units, *P*<0.05), while the Kir2.1 level was not significantly altered (0.30±0.03 vs. 0.27±0.05, *P*>0.05, Figure 7D).

To investigate whether exosomes (*i.e.* microvesicles secreted by mammalian cells containing instructive molecules including cytokines, mRNAs and miRNAs) were responsible for these effects, exosomes from the hMSC secretome (representing 28% hMSCs) were added to pure nrCMC cultures and refreshed every 2 days (Figure 8A). At day 9, optical mapping did not reveal any changes in APD_{90} (Figure 8B) or CV (Figure 8C) by adding hMSC-derived exosomes to nrCMC cultures, suggesting that the effect of the hMSC secretome on APD prolongation is primarily mediated by directly secreted factors, rather than by secreted microvesicle-associated factors.

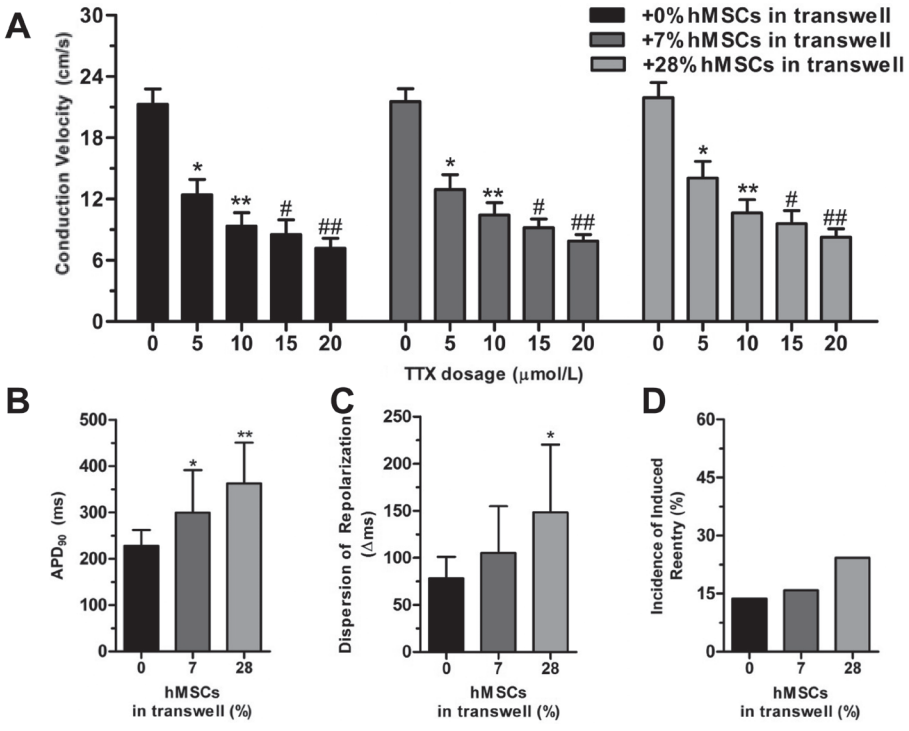

Figure 6. Paracrine mechanisms are responsible for hMSC-dependent prolongation of repolarization in myocardial cell cultures. (A) Dose-dependent effects of Nav1.5 blockade by TTX do not differ between control cultures and myocardial cell cultures exposed to the secretomes of different numbers of hMSCs. **P*<0.05 vs. 0 μmol/L TTX, ***P*<0.05 vs. 5 μmol/L TTX, #*P*<0.05 vs. 10 μmol/L TTX, ##*P*<0.05 vs. 15 μmol/L TTX. (B) Quantification of APD_{90}. **P*<0.05 vs. 0% and 28% hMSCs, ***P*<0.05 vs. 0% and 7%. (C) Quantification of dispersion of repolarization. **P*<0.05 vs. 0%. (D) Incidences of induced reentry in myocardial cell cultures exposed to transwells containing 0%, 7% or 28% of added hMSCs.

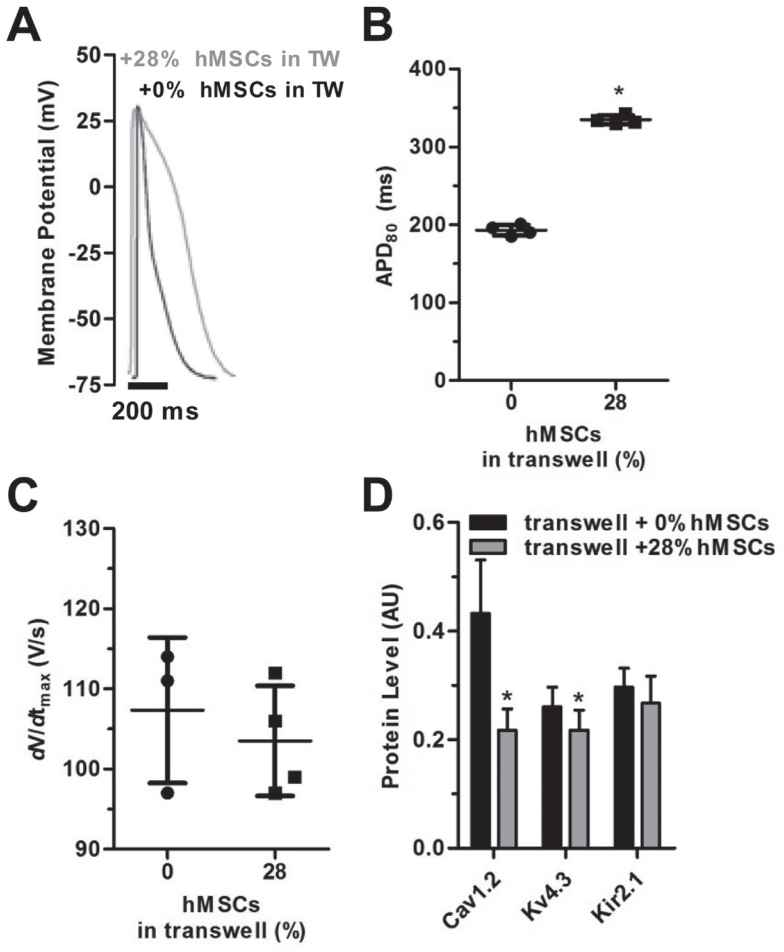

Figure 7. The hMSC secretome also affects nrCMCs at the cellular level. (A) Typical voltage traces of action potentials recorded in current-clamp experiments on nrCMCs subjected to the hMSC secretome and on control nrCMCs show (B) prolonged APD but (C) normal dV/dt_{max}. *P<0.05 vs. 0% hMSCs in transwells. (D) Quantification of western blot analyses of Cav1.2, Kv4.3 and Kir2.1 levels. Values are corrected for glyceraldehyde 3-phosphate dehydrogenase (GAPDH) levels. *P<0.05 versus transwell + 0% hMSCs. TW: transwell.

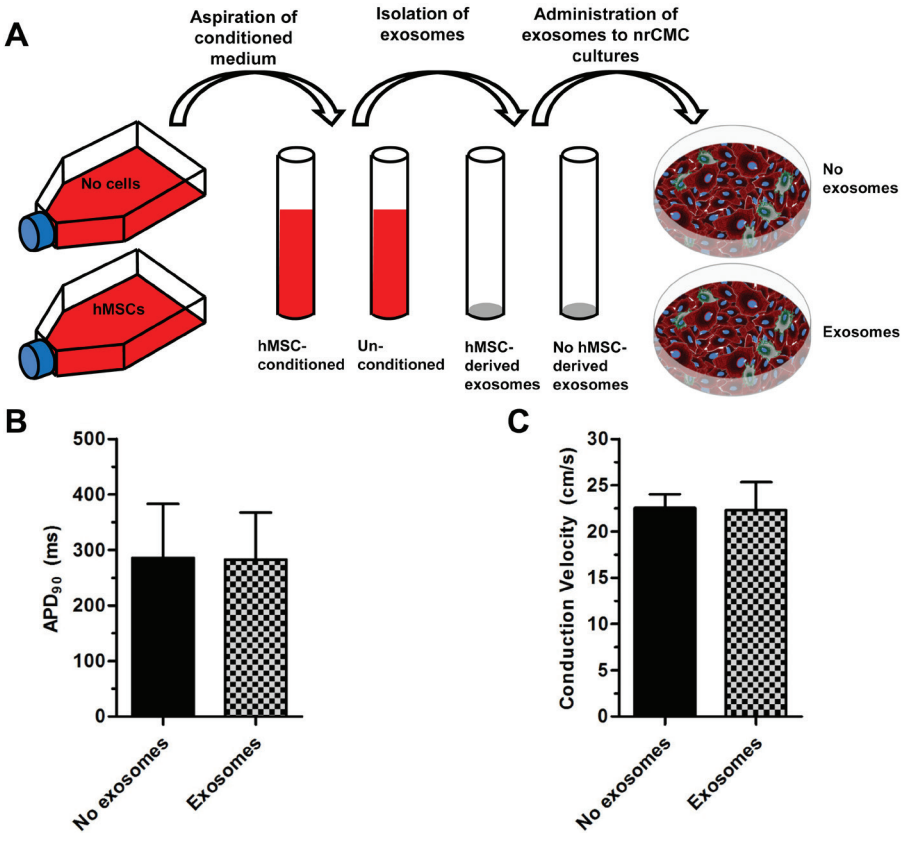

Figure 8. Human MSC-derived exosomes do not appear to exert pro-arrhythmic effects on nrCMCs. (A) Schematic overview of experiments investigating the pro-arrhythmic effects of hMSC-derived exosomes. (B) Adding exosomes to nrCMC cultures does not affect CV or (C) APD_{90} under optical mapping conditions.

DISCUSSION

This study has shown that (i) adult bone marrow-derived hMSCs contribute to APD dispersion, triggered activity and reentrant tachyarrhythmias in neonatal rat myocardial cell cultures; (ii) the pro-arrhythmic effects of hMSCs are mediated by two separate mechanisms, *i.e.* functional coupling of hMSCs with adjacent nrCMCs resulting in partial nrCMC depolarization and conduction slowing, and paracrine signaling of hMSCs to neighboring nrCMCs that slows nrCMC repolarization; and (iii) the number and distribution pattern of the MSCs in the myocardial cell cultures determine the type and severity of the arrhythmias.

EFFECT OF HMSC TRANSPLANTATION ON CARDIAC ELECTROPHYSIOLOGY

Whether and how cardiac cell therapy may increase the risk of ventricular arrhythmias remain topics of debate.[17-20] Gap-junctional coupling between transplanted cells and host cardiomyocytes appears to be essential for functional electrical integration, thereby preventing an increase in electrical heterogeneity, leading to arrhythmias.[21] Other studies have emphasized the role of cell alignment in electrical integration of transplanted cells in recipient myocardium and the potential pro-arrhythmic consequences of malalignment.[22] The number and distribution of donor cells in the host myocardium may also affect their arrhythmogenic potential.[11] However, very little is known about cell therapy-associated pro-arrhythmic mechanisms.

The current study demonstrates that both evenly spread and clustered hMSCs can exert pro-arrhythmic effects in myocardial cell cultures in a dose-dependent manner. However, the types of evoked arrhythmias depended on hMSC distribution pattern. By applying the hMSCs in a diffuse pattern, interactions with surrounding nrCMCs are maximized leading to increases in triggered activity and induced reentry incidence, while in myocardial cell cultures containing central clusters of hMSCs only the propensity towards reentry was increased. Triggered activity in diffuse co-cultures was associated with decreased repolarization reserve as APD shortening by opening of ATP-sensitive K^+-channels abolished such episodes, which together with pseudo-electrogram morphology, points to early afterdepolarizations as likely cause of triggered activity. As the P1075-treated cultures did not show any triggered activity, the concomitant APD shortening by P1075 did not lead to increased reentry incidence.[23]

The mechanism of early afterdepolarizations is considered to be reactivation of L-type calcium channels that linger within the window current due to a decreased repolarizing force.[23] As this mechanism is based on a highly complex and delicate balance between depolarizing and repolarizing forces that depends on activation and (de-)inactivation mechanics of ion channels, the absence of triggered activ-

ity in myocardial cell cultures containing clustered hMSCs can be explained by hMSC density-dependent skewing of action potential dynamics beyond the window current. The notion of density-dependent pro-arrhythmic effects of hMSCs is supported by findings of differences in CV and APD inside the 6-mm hMSC clusters in comparison to equal amounts of more diffusely integrated hMSCs. As hMSC clusters formed local zones of conduction delay and refractoriness, the cluster size-dependent increase in inducibility of reentry is most likely attributable to the increased possibility of spiral wave anchoring with increasing obstacle sizes.[24] Higher inducibility of reentry in cultures with diffusely spread hMSCs than in those containing clustered hMSCs indicates stronger pro-arrhythmic effects of widespread than of locally concentrated hMSC-nrCMC interactions.

ROLE OF HETEROCELLULAR COUPLING IN CONDUCTION SLOWING BY HMSCS

Conduction slowing is widely recognized as a pro-arrhythmic feature that increases the probability of wave front collision, partial conduction block and spiral wave formation.[23] In an earlier study, Chang *et al.* revealed that hMSCs slow conduction in myocardial cell cultures, presumably by electrotonic heterocellular interactions.[11] Two other studies showed the ability of hMSCs to overcome local conduction blocks by functional coupling to nrCMCs and passively and slowly conducting action potentials.[25,26] In the present study, we confirmed slowed conduction by hMSCs in myocardial cell cultures without anatomical conduction block. Importantly, hMSCs were shown to reduce nrCMC excitability as dV/dt_{max} and TTX sensitivity were decreased. Treatment of diffuse co-cultures with low doses of the gap-junctional uncoupler 2-ABP indicated that heterocellular coupling was the dominant mechanism responsible for the conduction-slowing effect of hMSCs. Although 2-APB, as most pharmacological agents, has other known effects, [27,28] these effects occur at higher dosages and cannot account for the increase in CV observed in Figure 2D. Partial heterocellular uncoupling increased CV in co-cultures and nrCMCs showed a more negative MDP and a higher action potential upstroke velocity, which are all indicative of partially restored excitability.[29] Heterocellular mechanical coupling was also investigated in the current study. Myofibroblasts were recently shown to exert pro-arrhythmic effects by providing a non-compliant mechanical resistance through their rigid cytoskeleton, which contains large amounts of αSMA and may thereby activate stretch-activated ion channels in nrCMCs.[30,31] However, the adult hMSCs used in this study did not express αSMA or N-cadherin in co-cultures with nrCMCs, which makes it unlikely that mechanical coupling plays a major role in hMSC-associated conduction slowing and arrhythmicity.

ROLE OF PARACRINE SIGNALING IN REPOLARIZATION SLOWING AND DISPERSION BY HMSCS

In cardiac arrhythmogenesis, prolonged repolarization times and dispersion of repolarization are considered crucial pro-arrhythmic factors for triggered activity and reentrant tachyarrhythmias.[23] Interestingly, while experiments with commercially obtained hMSCs reported no effect of these cells on repolarization or the incidence of triggered activity,[11] the present study provides evidence that clinically used hMSCs from ischemic heart disease patients in co-culture with nrCMCs can prolong repolarization time, increase repolarization dispersion and promote triggered activity, which is likely to be caused by spatial repolarization gradient steepening.[23] The mechanism of decreased repolarization reserve was elusive at first. In contrast to the effects of heterocellular uncoupling between nrCMCs and myofibroblasts,[32] decreasing heterocellular coupling between hMSCs and nrCMCs did not affect APD. However, it is becoming increasingly evident that the hMSC is a cell type with high paracrine activity that secretes a wide variety of directly secreted and exosome/microvesicle-associated factors associated with reverse remodeling and anti-inflammatory and pro-angiogenic activity.[33-35] These findings combined with the APD prolongation at the periphery of co-cultures containing clustered hMSCs, where there is no physical contact between hMSCs and nrCMCs raised the possibility that paracrine rather than electrotonic mechanisms are responsible for the decreased repolarization reserve. Indeed, experiments with hMSCs in transwell inserts to allow passage of the hMSC secretome without physical contact between hMSCs and nrCMCs, revealed hMSC dose-dependent increases in APD, dispersion of repolarization and inducibility of reentry in the nrCMCs seeded on the bottom of the transwell. As hMSC-derived exosomes did not significantly affect nrCMC APD, it is likely that APD prolongation in our model was based on directly secreted paracrine factors. Loss of biological activity of exosomes is unlikely, since they were purified using established procedures.[14,15] The current study has not provided any indication of pro-arrhythmic effects of exosomes purified from hMSC cultures. As exosomes may have a significant contribution to the therapeutic effects caused by the paracrine activity of MSCs, they might therefore represent a safer alternative to cell therapy for improving heart function.[16,36]

Paracrine activity of hMSCs has been associated with beneficial effects in *in vivo* models of cardiac remodeling.[33] A common feature of these models was the low engraftment rate of the hMSCs. As suggested in this study, higher hMSC engraftment rates might lead to increased production of paracrine factors tipping the balance from beneficial to adverse effects. Interestingly, paracrine signaling did not alter conduction or excitability, as the sensitivity of CV to Nav1.5 blockade by TTX remained the same between myocardial cell cultures exposed to the secretome of 0%, 7% or 28% hMSCs. It did, however, change the ion channel levels as revealed

by western blot analyses. In particular, Cav1.2 and Kv4.3 levels were significantly lowered by exposure to the hMSC secretome. While decreased Cav1.2 expression would theoretically shorten APD, lowered Kv4.3 expression prolongs APD by decreasing I_{to}.[37] Since APD prolongation was found both in optical mapping and patch-clamp experiments, the effect of lowered Kv4.3 expression appeared to be dominant in our cultures. The Kir2.1 level was not significantly altered in nrCMCs cultured below hMSC-containing transwell inserts, which is consistent with findings of intact excitability of nrCMCs exposed to the hMSC secretome. Although functional effects of altered ion channel expression are likely, more research is needed to be certain, since paracrine factors may also modulate the activity of proteins involved in cardiac impulse propagation by direct binding to these proteins or by inducing their post-translational modification. For example, a recent study by Desantiago showed that MSCs are able to increase I_{CaL} through the PI3K/Akt pathway.[38] Pinpointing the paracrine factors that are responsible for the pro-arrhythmic effects observed in our study and unraveling their mechanisms of action are subjects of future studies. The findings of the current study may raise cautionary concerns regarding the use of genetically-modified MSCs as biological pacemakers. [5] Such an approach relies on the premise that MSCs are electrically inert, other than their ability to couple to surrounding cells and achieve automaticity by electrotonic interactions. If MSCs modulate electrical behavior via secreted factors, using MSCs as pacemakers may have unintended APD prolonging effects and may increase the pro-arrhythmic risk.

Study Limitations

Due to ethical and technical limitations, cardiomyocytes of human adults could not be not investigated in this study. As an alternative, nrCMCs were used as these cells are available in large amounts and can be maintained in culture as contractile monolayers for the time period needed for mechanistic studies on stem cell engraftment. However, their ion channel expression profile and distribution of gap junctions differs from those of human adult CMCs. Therefore, the comparability of neonatal rat CMCs to adult and clinical situations may be limited. Nevertheless, 2-dimensional *in vitro* models of rat myocardial tissue have shown to be relevant for studying cardiac electrophysiology, by mimicking key electrophysiological processes in the intact heart.[39]

As the current model utilized healthy nrCMCs, the implications of current findings for disease models for stem cell therapy need to be investigated in future studies. To assess the consequences of this study for hMSC transplantation in the heart, our findings should be considered in the context of 3-dimensional, anisotropic myocardium.

CONCLUSION

In myocardial cell cultures, adult hMSCs slow conduction, prolong repolarization, increase spatial dispersion of repolarization and cause triggered activity and reentrant arrhythmias by different mechanisms. Electrotonic coupling of hMSCs to nrCMCs reduces excitability and thereby CV, while the paracrine factors that are directly secreted by hMSCs slows nrCMC repolarization. Thus, caution is warranted against potential pro-arrhythmic effects of MSC transplantation in cardiac tissue. The observation that the pro-arrhythmic activity of hMSCs in co-cultures with nrCMCs is strongly influenced by their number and distribution suggests that by controlling MSC engraftment rate and patterns the critical balance between therapeutic potential and hazardous risk of MSC therapy for cardiac diseases may be tipped in the right direction.

FUNDING

The financial contribution of the Netherlands Organisation for Scientific Research (NWO, Veni grant 91611070, D.A.P.), Dutch Heart Foundation (NHS, 2008/B119) and SMARTCARE of the BioMedical Materials program (project-P1.04) is gratefully acknowledged.

DISCLOSURE

None.

ACKNOWLEDGEMENTS

We thank H.J.F. van der Stadt, J.N. Schalij, A. van 't Hof, R. van Leeuwen and the technicians of the stem cell laboratory for their excellent technical support.

REFERENCES

1. Gerson SL. Mesenchymal stem cells: no longer second class marrow citizens. *Nat Med*. 1999;5:262-264.
2. Prockop DJ. Marrow stromal cells as stem cells for nonhematopoietic tissues. *Science*. 1997;276:71-74.
3. Grauss RW, Winter EM, van TJ, Pijnappels DA, Steijn RV, Hogers B, van der Geest RJ, de Vries AA, Steendijk P, van der Laarse A, Gittenberger-de Groot AC, Schalij MJ, Atsma DE. Mesenchymal stem cells from ischemic heart disease patients improve left ventricular function after acute myocardial infarction. *Am J Physiol Heart Circ Physiol*. 2007;293:H2438-H2447.
4. Pijnappels DA, Gregoire S, Wu SM. The integrative aspects of cardiac physiology and their implications for cell-based therapy. *Ann N Y Acad Sci*. 2010;1188:7-14.
5. Plotnikov AN, Shlapakova I, Szabolcs MJ, Danilo P, Jr., Lorell BH, Potapova IA, Lu Z, Rosen AB, Mathias RT, Brink PR, Robinson RB, Cohen IS, Rosen MR. Xenografted adult human mesenchymal stem cells provide a platform for sustained biological pacemaker function in canine heart. *Circulation*. 2007;116:706-713.
6. van Ramshorst J, Bax JJ, Beeres SL, Dibbets-Schneider P, Roes SD, Stokkel MP, de Roos A, Fibbe WE, Zwaginga JJ, Boersma E, Schalij MJ, Atsma DE. Intramyocardial bone marrow cell injection for chronic myocardial ischemia: a randomized controlled trial. *JAMA*. 2009;301:1997-2004.
7. Segers VF and Lee RT. Stem-cell therapy for cardiac disease. *Nature*. 2008;451:937-942.
8. Cheng K, Li TS, Malliaras K, Davis DR, Zhang Y, Marban E. Magnetic targeting enhances engraftment and functional benefit of iron-labeled cardiosphere-derived cells in myocardial infarction. *Circ Res*. 2010;106:1570-1581.
9. Segers VF and Lee RT. Biomaterials to enhance stem cell function in the heart. *Circ Res*. 2011;109:910-922.
10. Fukushima S, Varela-Carver A, Coppen SR, Yamahara K, Felkin LE, Lee J, Barton PJ, Terracciano CM, Yacoub MH, Suzuki K. Direct intramyocardial but not intracoronary injection of bone marrow cells induces ventricular arrhythmias in a rat chronic ischemic heart failure model. *Circulation*. 2007;115:2254-2261.
11. Chang MG, Tung L, Sekar RB, Chang CY, Cysyk J, Dong P, Marban E, Abraham MR. Proarrhythmic potential of mesenchymal stem cell transplantation revealed in an in vitro coculture model. *Circulation*. 2006;113:1832-1841.
12. National Institutes of Health. Guide for the Care and Use of Laboratory Animals. 1-1-2002. Ref Type: Statute
13. Askar SF, Ramkisoensing AA, Schalij MJ, Bingen BO, Swildens J, van der Laarse A, Atsma DE, de Vries AA, Ypey DL, Pijnappels DA. Antiproliferative treatment of myofibroblasts prevents arrhythmias in vitro by limiting myofibroblast-induced depolarization. *Cardiovasc Res*. 2011;90:295-304.
14. Lasser C, Eldh M, Lotvall J. Isolation and characterization of RNA-containing exosomes. *J Vis Exp*. 2012;e3037.
15. Thery C, Amigorena S, Raposo G, Clayton A. Isolation and characterization of exosomes from cell culture supernatants and biological fluids. *Curr Protoc Cell Biol*. 2006;Chapter 3:Unit.
16. Ranganath SH, Levy O, Inamdar MS, Karp JM. Harnessing the mesenchymal stem cell secretome for the treatment of cardiovascular disease. *Cell Stem Cell*. 2012;10:244-258.
17. Gepstein L. Electrophysiologic implications of myocardial stem cell therapies. *Heart Rhythm*. 2008;5:S48-S52.
18. Ly HQ and Nattel S. Stem cells are not proarrhythmic: letting the genie out of the bottle. *Circulation*. 2009;119:1824-1831.
19. Macia E and Boyden PA. Stem cell therapy is proarrhythmic. *Circulation*. 2009;119:1814-1823.

20. Smith RR, Barile L, Messina E, Marban E. Stem cells in the heart: what's the buzz all about? Part 2: Arrhythmic risks and clinical studies. *Heart Rhythm*. 2008;5:880-887.
21. Abraham MR, Henrikson CA, Tung L, Chang MG, Aon M, Xue T, Li RA, O' Rourke B, Marban E. Antiarrhythmic engineering of skeletal myoblasts for cardiac transplantation. *Circ Res*. 2005;97:159-167.
22. Pijnappels DA, Schalij MJ, Ramkisoensing AA, van TJ, de Vries AA, van der Laarse A, Ypey DL, Atsma DE. Forced alignment of mesenchymal stem cells undergoing cardiomyogenic differentiation affects functional integration with cardiomyocyte cultures. *Circ Res*. 2008;103:167-176.
23. Kleber AG and Rudy Y. Basic mechanisms of cardiac impulse propagation and associated arrhythmias. *Physiol Rev*. 2004;84:431-488.
24. Lim ZY, Maskara B, Aguel F, Emokpae R, Jr., Tung L. Spiral wave attachment to millimeter-sized obstacles. *Circulation*. 2006;114:2113-2121.
25. Beeres SL, Atsma DE, van der Laarse A, Pijnappels DA, van TJ, Fibbe WE, de Vries AA, Ypey DL, van der Wall EE, Schalij MJ. Human adult bone marrow mesenchymal stem cells repair experimental conduction block in rat cardiomyocyte cultures. *J Am Coll Cardiol*. 2005;46:1943-1952.
26. Pijnappels DA, Schalij MJ, van TJ, Ypey DL, de Vries AA, van der Wall EE, van der Laarse A, Atsma DE. Progressive increase in conduction velocity across human mesenchymal stem cells is mediated by enhanced electrical coupling. *Cardiovasc Res*. 2006;72:282-291.
27. Maruyama T, Kanaji T, Nakade S, Kanno T, Mikoshiba K. 2APB, 2-aminoethoxydiphenyl borate, a membrane-penetrable modulator of Ins(1,4,5)P3-induced Ca2+ release. *J Biochem*. 1997;122:498-505.
28. Harks EG, Camina JP, Peters PH, Ypey DL, Scheenen WJ, van Zoelen EJ, Theuvenet AP. Besides affecting intracellular calcium signaling, 2-APB reversibly blocks gap junctional coupling in confluent monolayers, thereby allowing measurement of single-cell membrane currents in undissociated cells. *FASEB J*. 2003;17:941-943.
29. Kizana E, Chang CY, Cingolani E, Ramirez-Correa GA, Sekar RB, Abraham MR, Ginn SL, Tung L, Alexander IE, Marban E. Gene transfer of connexin43 mutants attenuates coupling in cardiomyocytes: novel basis for modulation of cardiac conduction by gene therapy. *Circ Res*. 2007;100:1597-1604.
30. Rosker C, Salvarani N, Schmutz S, Grand T, Rohr S. Abolishing myofibroblast arrhythmogeneicity by pharmacological ablation of alpha-smooth muscle actin containing stress fibers. *Circ Res*. 2011;109:1120-1131.
31. Thompson SA, Copeland CR, Reich DH, Tung L. Mechanical coupling between myofibroblasts and cardiomyocytes slows electric conduction in fibrotic cell monolayers. *Circulation*. 2011;123:2083-2093.
32. Askar SF, Bingen BO, Swildens J, Ypey DL, van der Laarse A, Atsma DE, Zeppenfeld K, Schalij MJ, de Vries AA, Pijnappels DA. Connexin43 silencing in myofibroblasts prevents arrhythmias in myocardial cultures: role of maximal diastolic potential. *Cardiovasc Res*. 2012;93:434-444.
33. Timmers L, Lim SK, Arslan F, Armstrong JS, Hoefer IE, Doevendans PA, Piek JJ, El Oakley RM, Choo A, Lee CN, Pasterkamp G, de Kleijn DP. Reduction of myocardial infarct size by human mesenchymal stem cell conditioned medium. *Stem Cell Res*. 2007;1:129-137.
34. Williams AR and Hare JM. Mesenchymal stem cells: biology, pathophysiology, translational findings, and therapeutic implications for cardiac disease. *Circ Res*. 2011;109:923-940.
35. Lai RC, Chen TS, Lim SK. Mesenchymal stem cell exosome: a novel stem cell-based therapy for cardiovascular disease. *Regen Med*. 2011;6:481-492.
36. Lai RC, Arslan F, Lee MM, Sze NS, Choo A, Chen TS, Salto-Tellez M, Timmers L, Lee CN, El Oakley RM, Pasterkamp G, de Kleijn DP, Lim SK. Exosome secreted by MSC reduces myocardial ischemia/reperfusion injury. *Stem Cell Res*. 2010;4:214-222.

37. Hoppe UC, Marban E, Johns DC. Molecular dissection of cardiac repolarization by in vivo Kv4.3 gene transfer. *J Clin Invest*. 2000;105:1077-1084.
38. Desantiago J, Bare DJ, Semenov I, Minshall RD, Geenen DL, Wolska BM, Banach K. Excitation-contraction coupling in ventricular myocytes is enhanced by paracrine signaling from mesenchymal stem cells. *J Mol Cell Cardiol*. 2012;52:1249-1256.
39. Tung L and Zhang Y. Optical imaging of arrhythmias in tissue culture. *J Electrocardiol*. 2006;39:S2-S6.

SUPPLEMENTAL MATERIAL

ISOLATION, CULTURE AND CHARACTERIZATION OF HUMAN MESENCHYMAL STEM CELLS (HMSCS)

Human tissue samples were collected after having obtained written informed consent of the donors and with the approval of the medical ethics committee of Leiden University Medical Center (LUMC), where all investigations were performed. Investigations with human tissues conformed to the Declaration of Helsinki. Adult hMSCs were purified from leftover bone marrow (BM) samples derived from ischemic heart disease patients (n=4 donors). Briefly, the mononuclear cell fraction of the BM was isolated by Ficoll density gradient centrifugation, transferred to a 75-cm^2 cell culture flask (Becton Dickinson, Franklin Lakes, NJ) in standard hMSC culture medium (*i.e.* Dulbecco's modified Eagle's medium [DMEM; Invitrogen, Breda, the Netherlands] containing 10% fetal bovine serum [FBS; Invitrogen and incubated at 37°C in humidified 95% air/5%CO_2. Twenty-four h after seeding, the non-adherent cells were removed and the remaining hMSCs were expanded by serial passage using standard methods.[1] The hMSCs were characterized according to generally accepted criteria using flow cytometry for the detection of surface antigens and adipogenic and osteogenic differentiation assays to establish multipotency. Surface marker expression was examined after culturing the cells for at least 3 passages. Thereafter, the hMSCs were detached using a buffered 0.05% trypsin-0.02% EDTA solution (TE; Lonza, Vervier, Belgium), suspended in phosphate-buffered saline (PBS) containing 1% bovine serum albumin fraction V (BSA; Sigma-Aldrich Chemie, Zwijndrecht, the Netherlands) and divided in aliquots of 10^5 cells. Cells were then incubated for 30 min at 4°C with fluorescein isothiocyanate- or phycoerythrin-conjugated monoclonal antibodies (MAbs) directed against human CD105 (Ancell, Bayport, MN), CD90, CD73, CD45, CD34 or CD31 (all from Becton Dickinson). Labeled cells were washed three times with PBS containing 1% BSA and analyzed using a BD LSR II flow cytometer (Becton Dickinson). Isotype-matched control MAbs (Becton Dickinson) were used to determine background fluorescence. At least 10^4 cells per sample were acquired and data were processed using FACSDiva software (Becton Dickinson). Established differentiation assays were used to determine the adipogenic and osteogenic differentiation ability of the cells. Briefly, 5×10^4 hMSCs per well were plated in a 12-well cell culture plate (Corning Life Sciences, Amsterdam, the Netherlands) and exposed to adipogenic or osteogenic differentiation medium. Adipogenic differentiation medium consisted of MEM-plus (*i.e.* α-minimum essential medium [Invitrogen] containing 10% FBS, supplemented with insulin, dexamethason, indomethacin and 3-isobutyl-1-methylxanthine (all from Sigma-Aldrich Chemie) to final concentrations of 5 µg/mL, 1 µmol/L, 50 µmol/L and 0.5 µmol/L, respectively, and was refreshed every

3-4 days for a period of 3 weeks. Lipid accumulation was assessed by Oil Red O (Sigma-Aldrich Chemie) staining of the cultures (15 mg of Oil Red O per mL of 60% 2-propanol). Osteogenic differentiation medium consisted of MEM-plus containing 10 mmol/L β-glycerophosphate, 50 µg/mL ascorbic acid and 10 nmol/L dexamethason (all from Sigma-Aldrich Chemie) and was refreshed every 3-4 days for a period of 3 weeks. Osteogenic differentiation was evaluated by histochemical detection of alkaline phosphatase activity and calcium deposition. To measure alkaline phosphatase activity, cells were washed with PBS and subsequently incubated for 5 min with substrate solution (0.2 mg/mL a-naphthyl-1-phosphate [Sigma-Aldrich Chemie] 0.1 mol/L Tris-HCl [pH 8.9], 0.1 mg/mL magnesium sulfate and 0.6 mg/mL Fast Blue RR [Sigma-Aldrich Chemie]). Thereafter, calcium deposits were visualized by staining of the cells for 5 min with 2% Alizarin Red S (Sigma-Aldrich Chemie) in 0.5% NH_4OH (pH 5.5).

NEONATAL RAT VENTRICULAR CARDIOMYOCYTE (NRCMC) ISOLATION AND CULTURE

All animal experiments were approved by LUMC's animal experiments committee and conformed to the Guide for the Care and Use of Laboratory Animals, as stated by the US National Institutes of Health[2] (permit number: 10236). Isolation of nrCMCs from two-day-old neonatal Wistar rats was done essentially as described previously.[3] In brief, hearts were rapidly excised from isoflurane-anesthetized animals and minced into small pieces. After two sequential digestion steps with collagenase type I (450 units/mL; Worthington, Lakewood, NJ), a 75-min pre-plating step was performed to minimize the number of non-cardiomyocytes in the myocardial cell suspension. Next, the resulting cell suspension was passed through a nylon cell strainer with a mesh pore size of 70 µm (Becton Dickinson) to remove cell aggregates and, after counting, the cells were plated on fibronectin (Sigma-Aldrich Chemie)-coated round glass coverslips in 24-well cell culture plates (Corning Life Sciences, Amsterdam, the Netherlands) at a density of $1\text{-}4\times10^5$ cells/well depending on the experiment. To stop cell proliferation and to maintain the initial established ratios between cell types, cultures were incubated for 2 h with 10 µg/mL mitomycin-C (Sigma-Aldrich Chemie) at day 1 of culture. Culture medium was refreshed daily, except in experiments investigating paracrine effects. In these experiments, cells received fresh medium every 2 days to allow for sufficient exposure to paracrine factors. Cultures were refreshed with DMEM/Ham's F10 culture medium (1:1, v/v; both from Invitrogen) supplemented with 5% horse serum (HS; Invitrogen) and cultured in a humidified incubator at 37°C and 5% CO_2.

PREPARATION OF CO-CULTURES BETWEEN NRCMCS AND CLUSTERED OR DIFFUSELY SPREAD HMSCS

To investigate in an *ex vivo* model system the effects of myocardial engraftment of hMSCs in different patterns and doses on arrhythmogeneity, co-cultures of nrCMCs and hMSCs were prepared. To mimic a diffuse engraftment pattern, 4.0×10^5 nrCMCs with mixed with 2.8×10^4 (7%) or 1.12×10^5 (28%) hMSCs and added onto a fibronectin-coated glass coverslip in a well of a 24-well cell culture plate. To mimic a clustered engraftment pattern, the hMSCs were applied to the center of a glass coverslip in a circle with a diameter of 3 mm (2.8×10^4 cells) or of 6 mm (1.12×10^5 cells). To keep the hMSCs centered, rings with an outer diameter of 15 mm and an inner diameter of 3 or 6 mm were lasered in Parafilm M (Bemis Flexible Packaging, Neenah, WI, USA) using a PLS3.60 laser (Universal Lasersystems. Scottsdale, AZ). Next, these rings were sterilized with 70% ethanol and attached to fibronectin-coated coverslips. A drop of hMSC suspension was then applied to the center of each ring and the cells were allowed to adhere for at least 2 h. Finally, the rings of Parafilm M were removed and 4.0×10^5 nrCMCs were plated out on top of the hMSC cluster.

ELECTROPHYSIOLOGICAL MEASUREMENTS IN CO-CULTURES OF NRCMCS AND HMSCS

To facilitate the identification of hMSCs in co-cultures with nrCMCs, these cells were labeled with enhanced green fluorescent protein (GFP) using the vesicular stomatitis virus G protein-pseudotyped, self-inactivating human immunodeficiency virus type 1 vector CMVPRES,[4] essentially as described by van Tuyn *et al*.[5] At day 9 of culture, co-cultures of nrCMCs and GFP-labeled hMSCs in a diffuse or clustered pattern were subjected to whole-cell patch-clamp experiments in parallel to optical mapping experiments. Whole-cell current-clamp recordings were performed at 25°C using an L/M-PC patch-clamp amplifier (List Medical, Darmstadt, Germany) with 3 kHz filtering. Pipette solution contained (in mmol/L) 10 Na_2ATP, 115 KCl, 1 $MgCl_2$, 5 EGTA, 10 HEPES/KOH (pH 7.4). Tip resistance was 2.0 – 2.5 MΩ, and seal resistance >1 GΩ. The bath solution contained (in mmol/L) 137 NaCl, 4 KCl, 1.8 $CaCl_2$, 1 $MgCl_2$, 10 HEPES/KOH (pH 7.4). For data acquisition and analysis pClamp/Clampex8 software (Axon Instruments, Molecular Devices, Sunnyvale, CA) was used. Current-clamp recordings were performed in unlabeled nrCMCs adjacent to GFP-labeled hMSCs. For partial uncoupling experiments, nrCMCs were studied after 20 min of incubation with 2-aminoethoxydiphenyl borate (2-APB; Tocris, Ballwin, MO).

OPTICAL MAPPING

Electrophysiological parameters were determined by optical mapping as described previously.[6] In brief, nrCMC-hMSC co-cultures were loaded with 6 µmol/L of the

voltage-sensitive dye di-4-ANEPPS (Invitrogen) diluted in DMEM/Ham's F12 culture medium (Invitrogen) for 10 min at 37°C in humidified 95% air/5%CO_2. Subsequently, the culture medium was replaced by fresh DMEM/Ham's F12 and the cultures were optically mapped using the Micam Ultima-L optical mapping system (SciMedia USA, Costa Mesa, CA). Optical signals were recorded and analyzed using Brainvision Analyze 1108 (Brainvision, Tokyo, Japan). Cultures were electrically stimulated with a 10 ms pulse at ≥1.5× diastolic threshold and paced at 1 Hz (Multichannel systems, Reutlingen, Germany) to determine conduction velocity (CV) and action potential duration at 90% of full repolarization (APD_{90}), as well as dispersion of repolarization. Dispersion of repolarization was calculated as the maximal spatial difference in APD_{90} within the same culture. Areas of dispersion analysis were at least 4×4 pixels. Inducibility of reentry was tested by applying a bipolar, 14-Hz burst stimulation protocol. Reentry was defined as >2 consecutive circular activations. For partial uncoupling experiments, cultures were mapped before and after 20 min of incubation with 2-APB. The principle of partial uncoupling was based on the low connexin 43 (Cx43) plaque density at heterocellular hMSC-nrCMC junctions as compared to that at homocellular nrCMC-nrCMC junctions. This renders the gap junctional communication between nrCMCs and hMSCs more sensitive to uncoupling by 2 µmol/L of 2-APB than that between nrCMCs and nrCMCs. Thus, treatment of the co-cultures with 2-APB could effectively uncouple hMSCs from nrCMCs while preserving nrCMC reserves of Cx43 necessary for conduction. Although 2-APB may have other known effects, these are not expected to be active at the used dosages[7,8] and are not expected to increase conduction velocity.

To study the effects of fast sodium channel blockade, cultures were successively exposed to 5, 10, 15 and 20 µmol/L tetrodotoxin (TTX; Alomone Labs, Jerusalem, Israel) by stepwise increasing the drug concentration. The influence of APD on arrhythmicity was studied using the ATP-sensitive potassium channel opener P1075 (10 µmol/L; Tocris).

ANALYSIS OF MARKERS INVOLVED IN MECHANICAL AND ELECTRICAL COUPLING

Alpha smooth muscle actin (αSMA) and N-cadherin, proteins involved in mechanical coupling, were visualized by immunostaining as described previously.[1] In short, on day 9 after culture initiation, the co-cultures of nrCMCs and adult BM hMSCs were fixed on ice with 4% formaldehyde in PBS for 30 min, washed with PBS, permeabilized with 0.1% Triton X-100 in PBS for 5 min at 4°C and rinsed again with PBS. To decrease non-specific antibody binding, the cells were next incubated at room temperature with 0.1% donkey serum (Sigma-Aldrich Chemie) in PBS for 30 min. Thereafter, the co-cultures were incubated overnight at 4°C with an αSMA-specific mouse MAb (clone 1A4; A2547; Sigma-Aldrich Chemie) or with an N-cadherin-specific mouse MAb (clone ID-7.2.3; C3825; Sigma-Aldrich Chemie) diluted

1:400 and 1:100, respectively, in PBS containing 0.1% donkey serum. To distinguish nrCMCs from hMSCs, co-cultures were stained with a rabbit polyclonal antibody (PAb) recognizing the striated muscle-specific protein troponin I (H-170; Santa Cruz Biotechnology, Santa Cruz, CA; dilution 1:100). Binding of the primary antibodies to their target antigen was visualized using Alexa Fluor 568-conjugated donkey anti-mouse IgG and Alexa Fluor 488-conjugated donkey anti-rabbit IgG (both from Invitrogen) at dilutions of 1:200. hMSCs in the co-cultures were identified by labeling with a human lamin A/C-specific murine MAb (clone 636; Vector Laboratories, Burlingame, CA; dilution 1:200). Lamin A/C staining was visualized with Qdot 655-streptavidin conjugates (Invitrogen; dilution 1:200) after incubation of the cells with biotinylated goat anti-mouse IgG2b secondary antibodies (Santa Cruz Biotechnology; dilution 1:200). Nuclei were stained by incubating the cells for 10 min at room temperature with 10 μg/mL Hoechst 33342 (Invitrogen) in PBS.

The expression of the gap junctional protein Cx43, which plays an important role in the electrical coupling of nrCMCs, was also studied by immunocytological stainings. Co-cultures of nrCMCs and hMSCs were stained with a Cx43-specific rabbit PAb (C6219; Sigma-Aldrich Chemie) and with a mouse MAb recognizing sarcomeric α-actinin (clone EA53; Sigma-Aldrich Chemie; dilution 1:200). The primary antibodies were visualized using Alexa Fluor 568-coupled donkey anti-mouse IgG and Alexa Fluor 488-linked donkey anti-rabbit IgG secondary antibodies at dilutions of 1:200 (both Invitrogen). Again, the hMSCs in the co-cultures were identified by labeling with a human lamin A/C-specific murine MAb as described above. Nuclei were stained using a 10 μg/mL solution of Hoechst 33342 in PBS. Cells that went through the entire staining procedure but were not exposed to primary antibodies served as negative controls. A fluorescence microscope equipped with a digital color camera (Nikon Eclipse 80i; Nikon Instruments Europe, Amstelveen, the Netherlands) and dedicated software (NIS Elements [Nikon Instruments Europe] together with ImageJ [version 1.43; National Institutes of Health, Bethesda, MD]) were used for data analysis. ImageJ was used to determine the intensity of the Cx43-associated fluorescence in several randomly chosen, equally-sized border regions between hMSCs and nrCMCs and between adjoining nrCMCs. Fluorescent images of cells stained with the same antibody were always recorded with the same exposure time.

ANALYSIS OF FUNCTIONAL COUPLING

Dye transfer assays were used to directly determine functional heterocellular coupling between nrCMCs and GFP-positive hMSCs. Four days after cell isolation, nrCMC cultures with a density of 2×10^5 cells per well in a 12-well cell culture plate (Corning Life Sciences) were loaded with dye by incubation for 15 min with 4 mmol/L calcein red-orange AM (calcein; Invitrogen) in Hank's balanced

salt solution (Invitrogen). Thereafter, the cells were rinsed three times with PBS and were kept in the incubator in nrCMC culture medium supplemented with 2.5 mmol/L Probenecid (Invitrogen) for ³30 min before 2×10⁴ GFP-positive hMSCs (n=3 cultures for each of the 4 hMSC isolates) were added. Probenecid blocks organic anion transporters located in the plasma membrane thus preventing calcein efflux from the dye-loaded nrCMCs. Fluorescent images (³30 per group) were captured after 8 h and evaluated in a blinded manner. In all experimental groups, GFP-positive hMSCs surrounded by the same number of nrCMCs were analyzed. ImageJ was used to determine the intensity of the calcein-associated fluorescence in several randomly chosen, equally-sized subcellular regions for both the GFP-positive hMSCs and the adjoining nrCMCs. To correct for possible variations in calcein loading efficiency, the dye intensity in the GFP-positive hMSCs was expressed as a percentage of that in the surrounding nrCMCs. The percentage of calcein-positive cells among the GFP-labeled hMSCs was also determined by counting these cells in ³60 fields of view per experimental group.

ANALYSIS OF THE INFLUENCE OF PARACRINE FACTORS ON NRCMC CULTURES

To investigate the influence of hMSC paracrine factors on the electrophysiological properties of nrCMC cultures, transwell experiments were conducted. Mitomycin-C-treated adult hMSCs were seeded in 24-well plate transwell inserts (membrane diameter: 6.5 mm, surface area: 0.33 cm^2, membrane pore size: 0.4 µm; Corning Life Sciences). To allow direct comparison with the previously described co-culture experiments, the transwell inserts contained 2.8×10^4 or 1.12×10^5 hMSCs, which were placed above 4.0×10^5 mitomycin-C-treated nrCMCs seeded on fibronectin-coated coverslips. Control cultures consisted of nrCMC cultures with empty transwells, nrCMC cultures without transwells and nrCMC cultures with transwells containing 1.12×10^5 nrCMCs. All cultures included in these experiments were refreshed with standard nrCMC culture medium every 2 days. To confirm optical mapping results, patch-clamp experiments were also performed on nrCMCs exposed to the hMSC secretome using the transwell cell culture system and on nrCMCs of control cultures.

WESTERN BLOT ANALYSES

To investigate Cav1.2, Kir2.1 and Kv4.3 levels, western blot analyses were performed on whole-cell protein extracts obtained from nrCMC layers cultured under transwell inserts containing hMSCs or no cells. Proteins were extracted by homogenization using RIPA buffer (150 mM NaCl, 1% Nonidet P-40, 0.5% sodium deoxycholate, 0.1% SDS, 50 mM Tris-HCl [pH 8.0] supplemented with protease inhibitors [cOmplete, Mini Protease Inhibitor Cocktail Tablets from Roche Diagnostics Nederland, Almere, the Netherlands]). At least 5 samples comprised of ≥2 cultures per

group were used. Total protein (10 µg/lane) was loaded onto NuPage 10% Bis-Tris gels (Invitrogen) and electrophoresis was performed for 2 h at 150 V, after which proteins were transferred to Hybond-P polyvinylidene difluoride membranes (GE healthcare, Diegem, Belgium) overnight using a wet blotting system. After blocking for 1 h at room temperature with 10 mmol/L Tris-HCl (pH7.6), 0.05% Tween-20 and 150 mmol/L NaCl (TBST) containing 5% BSA, the membranes were incubated for 1 h at room temperature with primary antibodies diluted in TBST-5% BSA. The primary antibodies were affinity-purified rabbit anti-mouse Cav1.2 (ACC-003; Alomone labs; dilution: 1/500), rabbit anti-human Kir2.1 (APC-026; Alomone labs; dilution: 1/1,000) and rabbit anti-rat Kv4.3 (P0358; Sigma-Aldrich Chemie; dilution: 1/1,000). For normalization purposes, a mouse MAb recognizing the housekeeping protein glyceraldehyde-3-phosphate dehydrogenase (GAPDH; clone 6C5; MAB374; Merck Millipore, Billerica, MA; dilution 1:50,000) was used. Following three 15-min washing steps with TBST, the membranes were incubated with appropriate horseradish peroxidase (HRP)-conjugated rabbit or mouse IgG-specific goat secondary antibodies (sc-3837 and sc-2005 from Santa Cruz Biotechnology, Santa Cruz, CA) diluted 15,000-fold in TBST-5% BSA. Following additional washing steps, blots were developed using SuperSignal West Femto Maximum Sensitivity Substrate (Thermo Scientific, Rockford, IL). The chemiluminescence signals were captured using a ChemiDoc XRS imaging system (Bio-Rad Laboratories, Veenendaal, the Netherlands).

EXOSOME EXPERIMENTS

To investigate their pro-arrhythmic effects, exosomes from the hMSC secretome were isolated under sterile conditions using previously established procedures.[9,10] Human MSCs were seeded into porcine skin gelatin type A (Sigma-Aldrich Chemie)-coated cell culture flasks with a surface area of 75 cm^2 (1.8 million cells per flask). As control, equal-sized gelatin-coated flasks without cells were used. Every 2 days, culture medium was collected from the flasks and spun for 10 minutes at 303 × *g* to remove cellular debris. The supernatant was transferred to clean tubes and stored shortly at 4°C. Subsequently, supernatants were centrifuged for 30 min at 4°C and 10,000 × *g* in a precooled Optima L-70K ultracentrifuge (Beckman Coulter Nederland, Woerden, the Netherlands) for another debris removal step. Next, supernatants were filtered through Millex 0.45-µm pore size polyethersulfone syringe filters (Merck Millipore) and spun for 60 min at 4°C and 100,000 × *g* to pellet the exosomes. Exosomes were resuspended in ice-cold PBS by gentle agitation for 2 h at 4°C. Exosomes were stored at -80°C until later use.

To study the effects of the hMSC-derived exosomes on the electrical properties of nrCMCs, 4×10^5 of these cells were added to single wells of a 24-well cell culture plate onto a fibronectin-coated glass coverslip. The resulting nrCMC cultures were given fresh medium with or without exosomes every 2 days. Exosomes were added to the medium in a quantity calculated to approximate the amount of exosomes in the hMSC secretome during the transwell experiments (Amount of hMSCs per flask / amount of hMSCs in transwells (*i.e.* 1.12 x10^5 cells) = dilution of exosome stock needed per nrCMC culture). After 9 days of culture, nrCMC cultures were subjected to optical mapping for electrophysiological investigation by a blinded researcher.

REFERENCES

1. Ramkisoensing AA, Pijnappels DA, Askar SF, Passier R, Swildens J, Goumans MJ, Schutte CI, de Vries AA, Scherjon S, Mummery CL, Schalij MJ, Atsma DE. Human embryonic and fetal mesenchymal stem cells differentiate toward three different cardiac lineages in contrast to their adult counterparts. *PLoS One*. 2011;6:e24164.
2. National Institutes of Health. Guide for the Care and Use of Laboratory Animals. 1-1-2002.
3. Pijnappels DA, Schalij MJ, van TJ, Ypey DL, de Vries AA, van der Wall EE, van der Laarse A, Atsma DE. Progressive increase in conduction velocity across human mesenchymal stem cells is mediated by enhanced electrical coupling. *Cardiovasc Res*. 2006;72:282-291.
4. Seppen J, Rijnberg M, Cooreman MP, Oude Elferink RP. Lentiviral vectors for efficient transduction of isolated primary quiescent hepatocytes. *J Hepatol*. 2002;36:459-465.
5. van Tuyn J, Pijnappels DA, de Vries AA, van der Velde-van Dijke I, Knaan-Shanzer S, van der Laarse A, Schalij MJ, Atsma DE. Fibroblasts from human postmyocardial infarction scars acquire properties of cardiomyocytes after transduction with a recombinant myocardin gene. *FASEB J*. 2007;21:3369-3379.
6. Askar SF, Ramkisoensing AA, Schalij MJ, Bingen BO, Swildens J, van der Laarse A, Atsma DE, de Vries AA, Ypey DL, Pijnappels DA. Antiproliferative treatment of myofibroblasts prevents arrhythmias in vitro by limiting myofibroblast-induced depolarization. *Cardiovasc Res*. 2011;90:295-304.
7. Maruyama T, Kanaji T, Nakade S, Kanno T, Mikoshiba K. 2APB, 2-aminoethoxydiphenyl borate, a membrane-penetrable modulator of Ins(1,4,5)P3-induced Ca2+ release. *J Biochem*. 1997;122:498-505.
8. Harks EG, Camina JP, Peters PH, Ypey DL, Scheenen WJ, van Zoelen EJ, Theuvenet AP. Besides affecting intracellular calcium signaling, 2-APB reversibly blocks gap junctional coupling in confluent monolayers, thereby allowing measurement of single-cell membrane currents in undissociated cells. *FASEB J*. 2003;17:941-943.
9. Lasser C, Eldh M, Lotvall J. Isolation and characterization of RNA-containing exosomes. *J Vis Exp*. 2012;e3037.
10. Thery C, Amigorena S, Raposo G, Clayton A. Isolation and characterization of exosomes from cell culture supernatants and biological fluids. *Curr Protoc Cell Biol*. 2006;Chapter 3:Unit.

SUPPLEMENTAL FIGURES

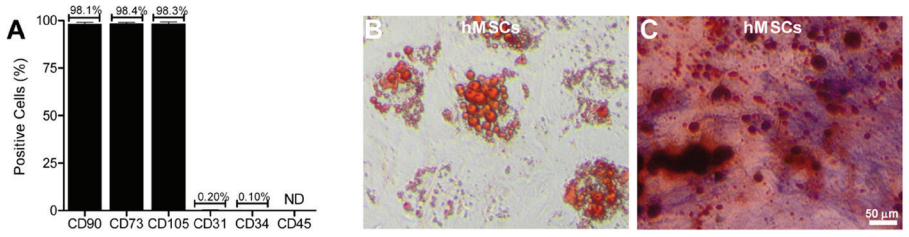

Supplemental figure 1. Characterization of adult BM hMSCs. (A) Flow cytometric analyses showed abundant surface expression of the MSC markers CD90, CD73 and CD105 and hardly any surface expression of the hematopoietic cell markers CD34 and CD45 or the endothelial cell marker CD31. Percentages are means of ≥4 measurements. ND is not detected. (B) Adipogenic differentiation was visualized by the presence of Oil Red O-stained fat vacuoles. (C) Calcium depositions and alkaline phosphatase activity were present after osteogenic differentiation of the hMSCs.

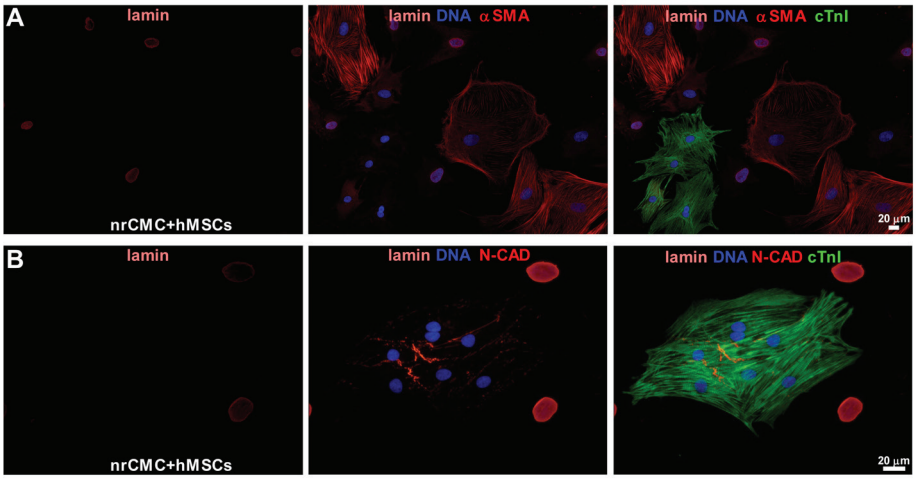

Supplemental figure 2. Analyse of markers involved in mechanical coupling. (A) Immunocytological staining showed no expression of alpha smooth muscle actin (aSMA; orange/red) by adult BM hMSCs in co-culture with nrCMCs. (B) Also, no N-cadherin (indicated as N-CAD; orange/red), was detected at contact areas between hMSCs and nrCMCs. hMSCs were detected using an antibody directed against human-specific lamin A/C (red), while nrCMCs were identified using an antibody directed against cardiac troponin I (cTnI; green). Nuclei were stained with the DNA-binding fluorochrome Hoechst 33342.